Surface critical behaviour of an O(n) loop model related to two Manhattan lattice walk problems

1995 J. Phys. A: Math. Gen. 28 839

(http://iopscience.iop.org/0305-4470/28/4/011)

J. Phys. A: Math. Gen. 28 (1995) 839–852. Printed in the UK

Surface critical behaviour of an O(n) loop model related to two Manhattan lattice walk problems

M T Batchelor†‖, A L Owczarek‡¶, K A Seaton§ and C M Yung†

† Department of Mathematics, Australian National University, Canberra, ACT 0200, Australia
‡ Department of Mathematics, The University of Melbourne, Parkville, Victoria 3052, Australia
§ School of Mathematics, La Trobe University, Bundoora, Victoria 3083, Australia

Received 15 September 1994, in final form 31 October 1994

Abstract. We find and discuss the scaling dimensions of the branch 0 manifold of the Nienhuis O(n) loop model on the square lattice, concentrating on the surface dimensions. The results are extracted from a Bethe ansatz calculation of the finite-size corrections to the eigenspectrum of the six-vertex model with free boundary conditions. These results are especially interesting for polymer physics at two values of the crossing parameter λ. Interacting self-avoiding walks on the Manhattan lattice at the collapse temperature ($\lambda = \pi/3$) and Hamiltonian walks on the Manhattan lattice ($\lambda = \pi/2$) are discussed in detail. Our calculations illustrate the importance of examining both odd and even strip widths when performing finite-size correction calculations to obtain scaling dimensions.

1. Introduction

Recently, work [1] on interacting self-avoiding walks (ISAW) on the Manhattan lattice (see figure 1) has given a set of scaling dimensions, except one, in accord with those of Duplantier and Saleur [2] for the problem of bulk θ-point polymers in two dimensions. This work also gave exponents for the surface transitions which are in complete accord with those of Vanderzande, Seno and Stella [3, 4]. These results arise from simulations of kinetic growth walks on the Manhattan lattice [1]. There is a configurational mapping from kinetic growth walks (MKGW) on the Manhattan lattice to the static ISAW problem on that lattice [5, 6]. The work in [1] extends Bradley's mapping [6] to the surface problem and the very existence of the mapping determines some of the surface exponents. One can understand heuristically why the single scaling dimension is different simply because the Manhattan lattice restricts configurations to those that can only trap by loop formation. Otherwise, these results demonstrate a θ-point model, without the spurious next-nearest neighbour interactions, that essentially possesses the same critical behaviour as the Duplantier–Saleur model.

It was also pointed out in [1] that an exactly solvable O(n) loop model recently examined in [7] has, in the limit $n \to 0$, precisely the same configurations as those of (isolated) closed trails on the L-lattice and hence self-avoiding polygons on the Manhattan lattice. This arises through a site-to-bond mapping of trails on the square lattice that turn at each vertex (which are the configurations of the branch 0 O(n) loop model) to the walks on the Manhattan lattice (see figure 2). The relevant bulk scaling dimensions calculated in [7] were those

‖ Email: murray.batchelor@anu.edu.au
¶ Email: aleks@mundoe.maths.mu.oz.au

0305-4470/95/040839+14$19.50

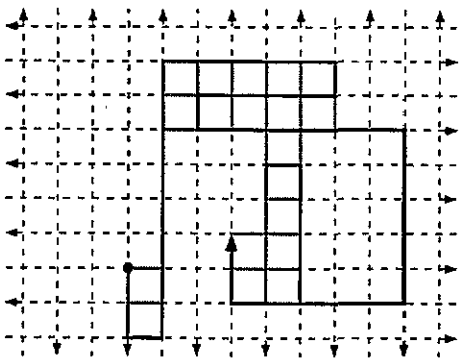

Figure 1. A self-avoiding walk on the Manhattan lattice with nearest-neighbour interactions identified.

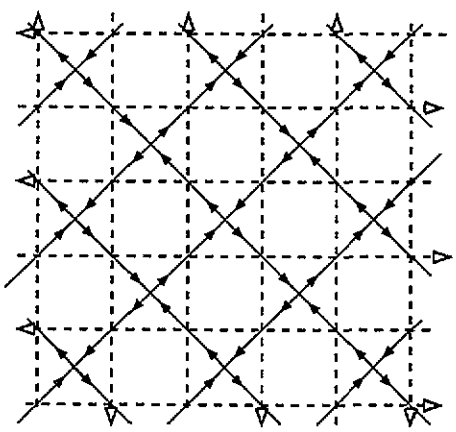

Figure 2. A section of the Manhattan lattice (directed broken lines) covering the L-lattice (directed full lines). Each directed bond of the L-lattice is mapped (uniquely) to a site of the Manhattan lattice. The loop model is defined on the L-lattice.

found in [1]. The confirmation of the scaling dimensions in the exactly solvable model was through the calculation of finite-size corrections to the eigenspectrum, utilizing the Bethe ansatz solution.

It is then appropriate to perform a similar finite-size correction calculation on the loop model with appropriate boundary conditions to give the surface scaling dimensions. However, the bulk calculation was completed by applying the Bethe ansatz method directly to an equivalent six-vertex model and the equivalence was shown through the use of the Temperley–Lieb algebra. In this paper we extend the mapping of the Manhattan collapsing polymer/MKGW to the loop model, and the loop model to the six-vertex model, in the case of surfaces. Instead of the algebraic equivalence of the six-vertex model and the loop model [7] we demonstrate a configurational equivalence. We then perform the proposed Bethe ansatz calculation in a manner that is an extension of [8] and related works. This gives us the surface scaling dimensions of the collapse problem and, indeed, confirms the results of [1]. In doing so we make certain observations about the relationship between scaling dimensions calculated in one model and another 'equivalent' model and about the necessity

of carrying out the Bethe ansatz calculation on both odd and even strip widths. We also note that in these calculations we make use of an exact configurational mapping between the dilute O(n) model and a dense O($n+1$) model.

The mapping of the Manhattan ISAW problem (at the θ-point) to the six-vertex model occurs for a particular value of the six-vertex 'crossing' parameter $\lambda = \pi/3$. On the other hand, most of our Bethe ansatz results and related comments are true for general λ. Another value of the crossing parameter that is of interest is $\lambda = \pi/2$. The six-vertex model here maps to a dense O(n) loop model with $n = 0$. This, in turn, can be mapped to the problem of Hamiltonian or fully packed walks on the Manhattan lattice. This last problem has received extensive treatment [9–11]. It is believed to be equivalent to the problem of dense polymers and conjectured that the Manhattan lattice constraint is irrelevant. We remark on these conjectures in the light of our results and recent work on other fully packed problems.

The paper is set out as follows. In section 2 we survey the existing results for the bulk problem. Section 3 defines the models of interest with free surfaces and describes the mapping from the loop model to the six-vertex model. The Bethe ansatz calculation of the finite-size corrections to the eigenspectrum is sketched. The results of numerical diagonalisation of the loop models and a related 15-vertex model are compared to those of the six-vertex model. The results of all these calculations and mappings are summarized and discussed in the concluding section.

2. Nienhuis O(n) loop model in the bulk

The model suggested by Nienhuis [12, 13], examined in [13, 7] and shown to be equivalent [1] to interacting walks on the Manhattan lattice at the θ-temperature, is a seven-vertex loop model on the square lattice derived from the O(n) model. Batchelor [7] has identified a set of bulk scaling dimensions x_j^{b} of this O(n) model as

$$x_j^{\mathrm{b}} = \frac{[j^2(\pi-\lambda)^2 - \lambda^2]}{2\pi(\pi-\lambda)} \tag{2.1}$$

with $j = 1, 2, \ldots$ and the central charge as

$$c^{\mathrm{b}} = 1 - \frac{6\lambda^2}{\pi(\pi-\lambda)}. \tag{2.2}$$

These were found from the known six-vertex results extracted via finite-size corrections to the eigenspectrum on strips that are an even number of edges wide. These are geometric exponents of the O(n) model and relate to the so-called watermelon correlators; the scaling dimension x_j describes the decay of the correlation function constructed from $2j$ self-avoiding paths [14].

These values fit into the Kac table as

$$x_j^{\mathrm{b}} = 2\Delta(0, j) \tag{2.3}$$

where Δ is given by the Kac formula (for instance see [15])

$$\Delta(p, q) = \frac{[p(h+1) - qh]^2 - 1}{4h(h+1)} \tag{2.4}$$

with h related to the central charge as

$$c^{\mathrm{b}} = 1 - \frac{6}{h(h+1)} \tag{2.5}$$

and so

$$h + 1 = \pi/\lambda. \tag{2.6}$$

Hence, for $n = 0$ we have $h = 2$ and $c^{\mathrm{b}} = 0$ with

$$x_j^{\mathrm{b}} = \frac{4j^2 - 1}{12}. \tag{2.7}$$

Note that

$$x_1^{\mathrm{b}} = \tfrac{1}{4} \qquad \text{and} \qquad x_2^{\mathrm{b}} = \tfrac{5}{4} \tag{2.8}$$

and since these satisfy $x \leqslant 2$ they are associated with the relevant scaling fields. The Kac table is often restricted by assuming that $h \geqslant 3$, $0 < p < h$ and $0 < q \leqslant h$ since the associated field theories are unitary. This is not the case here [16] and so the system's scaling dimensions lie outside the normal restrictions.

For odd strip widths [7] the central charge calculated from the free energy is given as

$$c^{b,\mathrm{odd}} = -\frac{1}{2} + \frac{3\lambda}{2\pi} \tag{2.9}$$

and the smallest scaling dimensions are 0 and $1 - \lambda/\pi$. (The full series is $x_j^{b,\mathrm{odd}} = (j^2 + j)(\pi - \lambda)/2\pi$ with $j = 0, 1, \ldots$.) However, if one is interested in the mappings to the Manhattan lattice, odd strip widths are unphysical since they cannot form periodic boundary conditions. We come back to this point in the discussion but point out now that for open boundaries this restriction does not apply.

3. Integrable loop models on the square lattice with open boundaries

Let $\mathcal{L}$ be the lattice depicted in figure 3, which we call the square lattice with open boundaries. A loop model on $\mathcal{L}$ has partition function

$$Z_{\mathrm{loop}} = \sum_{\mathcal{G}} \rho_1^{m_1} \ldots \rho_{13}^{m_{13}} n^P \tag{3.1}$$

where the sum is over all configurations $\mathcal{G}$ of non-intersecting closed loops which cover some (or none) of the edges of $\mathcal{L}$. The possible configurations at each vertex are shown in figure 4, with the one of type i carrying a Boltzmann weight ρ_i. In the configuration $\mathcal{G}$, m_i is the number of occurrences of the vertex of type i while P is the total number of closed

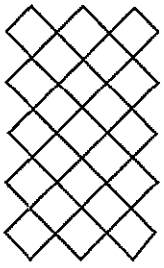

Figure 3. The lattice $\mathcal{L}$, of 'extent' M and N ($M = 10$ and $N = 6$ in the figure drawn) in the vertical and horizontal directions, respectively. Boundary conditions are open in the horizontal direction and periodic in the vertical.

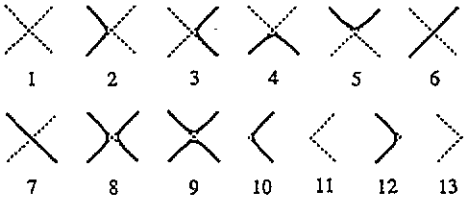

Figure 4. Allowed vertices for the loop model with partition function Z_{loop}. Vertex i carries Boltzmann weight ρ_i.

loops of fugacity n. Much work has been done on models where the boundary weights ρ_{10} to ρ_{13} are absent (see e.g. [12, 17]).

Instances where the loop model is integrable are known. Such important cases can be related to more well known integrable vertex models via the (loop model)-to-(vertex model) mapping [18, 12, 17]. This involves first assigning orientations to the loops in $\mathcal{G}$. The explicit closed loop counting in Z_{loop}, which is a non-local procedure, can be eliminated by introducing a weight $s(s^{-1})$ for each left (right) turn along an oriented loop if s is chosen so that

$$n = s^4 + s^{-4}. \tag{3.2}$$

The loop model partition function then becomes equivalent to a (three-state) vertex model partition function

$$Z_{\text{vertex}} = \sum_{\text{configs}} \prod_{\text{vertices}} (\text{Boltzmann weights}). \tag{3.3}$$

The weights for this vertex model are functions of ρ_i, s and, in general, gauge factors a, b, c and d (the presence of which leave the partition function unchanged). The allowed vertex states are shown in figures 5 and 6, with the bulk weights being w_i and the left and right boundary weights w_i^{L} and w_i^{R}, respectively. For a dense loop model (where only ρ_8, ρ_9, ρ_{10} and ρ_{12} are non-zero) the relations between the loop weights ρ_i and the vertex weights are explicitly given by

$$w_{14} = w_{15} = \rho_8$$
$$w_{16} = w_{17} = \rho_9$$

$$
\begin{aligned}
w_{18} &= (\rho_8 s^2 + \rho_9 s^{-2})\frac{ac}{bd} \\
w_{19} &= (\rho_8 s^{-2} + \rho_9 s^2)\frac{bd}{ac} \\
w_1^{\mathrm{L}} &= \rho_{10} s^{-1}\frac{1}{(ac)} \\
w_3^{\mathrm{L}} &= \rho_{10} s\frac{1}{(bd)} \\
w_1^{\mathrm{R}} &= \rho_{12} s(ac) \\
w_3^{\mathrm{R}} &= \rho_{12} s^{-1}(bd).
\end{aligned} \tag{3.4}
$$

Integrable vertex models on $\mathcal{L}$ can be found via the coordinate Bethe ansatz [8, 19] or via Sklyanin's extension of the quantum inverse scattering method [20–22]. Given such an integrable vertex model, there may or may not be a corresponding loop model [22].

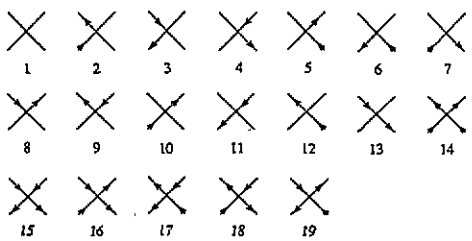

Figure 5. Allowed bulk vertices for integrable two- and three-state vertex models studied in this paper. Vertex i has an associated Boltzmann weight w_i.

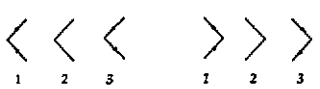

Figure 6. Allowed boundary vertices for the vertex models concerned. The left (respectively, right) boundary vertices have Boltzmann weights w_i^{L} (respectively, w_i^{R}).

3.1. The dense O(n) loop model

For the six-vertex model on $\mathcal{L}$ solved in [8] there *is* an associated loop model, the dense O(n) model with partition function

$$
Z_{\mathrm{dense}} = \sum_{\mathcal{G}} \rho_8^{m_8}\rho_9^{m_9}\rho_{10}^{m_{10}}\rho_{12}^{m_{12}} n^P \tag{3.5}
$$

where

$$
\rho_8 = 1 \qquad \rho_9 = \frac{\sin(u)}{\sin(\lambda - u)} \qquad \rho_{10} = \rho_{12} = 1 \tag{3.6}
$$

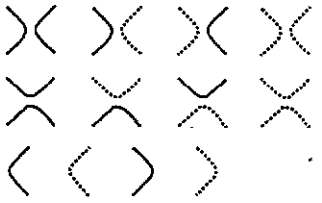

Figure 7. *Allowed vertices for the two-colour loop model. Colours 1 and 2 are indicated by* full and broken curves, respectively. The Boltzmann weights are, respectively, $\sin(\lambda-u)$, $\sin u$ and 1 for vertices in the three rows.

and loop fugacity $n = 2\cos\lambda$. The weights for the six-vertex model on $\mathcal{L}$ given in [8] can be recovered from (3.4) by choosing the gauge factors so that $ac = s^{-1}$ and $bd = s^{-1}$ (the variable t in [8] is $t = s^2$) with $s^4 = e^{i\lambda}$. With a different gauge choice, where $ac = s^{-1}$ and $bd = s$, the weights can be written as

$$w_{14}, w_{15}, w_{16}, w_{17}, w_{18}, w_{19} = (1, 1, x, x, 1 + xe^{-i\lambda}, 1 + xe^{i\lambda})$$
$$w_1^{\mathrm{L}}, w_3^{\mathrm{L}}, w_1^{\mathrm{R}}, w_3^{\mathrm{R}} = (1, 1, 1, 1) \tag{3.7}$$

with $x = \sin(u)/\sin(\lambda-u)$. The 'diagonal-to-diagonal' transfer matrix $t_{\mathrm{D}}(u)$ for this model has eigenvalue [8]

$$\Lambda(u) = \prod_{j=1}^{m} \frac{\sinh[u_j + \frac{1}{2}(u+\lambda)]\sinh[u_j - \frac{1}{2}(u+\lambda)]}{\sinh[u_j + \frac{1}{2}(u-\lambda)]\sinh[u_j - \frac{1}{2}(u-\lambda)]} \tag{3.8}$$

where $u_j (j = 1, 2, \ldots, m)$ are roots of the Bethe ansatz equations

$$\left[\frac{\sinh[u_j + \frac{1}{2}(u-\lambda)]\sinh[u_j - \frac{1}{2}(u+\lambda)]}{\sinh[u_j + \frac{1}{2}(u+\lambda)]\sinh[u_j - \frac{1}{2}(u-\lambda)]}\right]^N = \prod_{\substack{k=1 \\ \neq j}}^{m} \frac{\sinh(u_k + u_j - i\lambda)\sinh(u_k - u_j - i\lambda)}{\sinh(u_k + u_j + i\lambda)\sinh(u_k - u_j + i\lambda)}. \tag{3.9}$$

3.2. The dilute O(n) loop model

There is another loop model connected with the six-vertex model, the so-called dilute (i.e. not all edges of $\mathcal{L}$ are covered) O(n) model. This model has a partition function Z_{dilute} equivalent to Z_{dense} but involves different loop weights. The equivalence can be shown [23] by mapping Z_{dense} to a two-colour dense loop model [17] with fugacities n_1 and n_2 such that $n_1 + n_2 = n$. The Boltzmann weights of this two-colour loop model are given in figure 7. Setting $n_2 = 1$ and summing over the second colour one arrives at Z_{dilute} with weights

$$\rho_1 = 1 + x$$
$$\rho_2 = \rho_3 = \rho_8 = 1$$
$$\rho_4 = \rho_5 = \rho_9 = x$$
$$\rho_{10} = \rho_{11} = \rho_{12} = \rho_{13} = 1. \tag{3.10}$$

The Bethe ansatz solution is the same as for the dense model, but the loop fugacity n (in the mapping this is n_1) is now given by $n = 2\cos\lambda - 1$.

With a suitable gauge choice, this loop model can be mapped onto a three-state vertex model with weights:

$$w_1, w_2, w_3, w_4, w_5, w_6, w_7 = (1+x, 1, 1, 1, 1, xs^2, xs^{-2})$$
$$w_8, w_9, w_{14}, w_{15}, w_{16}, w_{17}, w_{18}, w_{19} = (xs^2, xs^{-2}, 1, 1, x, x, 1+xs^{-4}, 1+xs^4)$$
$$w_1^{\mathrm{L}}, w_2^{\mathrm{L}}, w_3^{\mathrm{L}}, w_1^{\mathrm{R}}, w_2^{\mathrm{R}}, w_3^{\mathrm{R}} = (1, 1, 1, 1, 1, 1) \tag{3.11}$$

where $x = \sin(u)/\sin(\lambda - u)$ and s is chosen so that $s^4 + s^{-4} = 2\cos\lambda - 1$. The bulk weights can be shown to lead to the Temperley–Lieb relations, again with $\sqrt{Q} = 2\cos\lambda$.

We note that for both the dense and dilute loop models there is freedom to multiply the surface weights by an overall factor ρ_s^{L} at the left boundary and by ρ_s^{R} at the right boundary. This introduces the freedom of equivalent surface weights w_s^{L} and w_s^{R} in (3.7) and (3.11). The overall effect is to introduce a multiplicative factor $w_s^{\mathrm{L}} w_s^{\mathrm{R}}$ on the right-hand side of the eigenvalue expression (3.8).

3.3. Manhattan walks

The dilute loop model is easily related to closed L-lattice trails interacting with a surface and hence to Manhattan walks near a surface. In the limit $n = 0$ for the isotropic ($u = \lambda/2$) dilute loop model ($\lambda = \pi/3$) one can consider an isolated loop. First we normalize the weights so that an empty vertex has weight 1. The configuration of this loop is that of a trail on the L-lattice. The vertex weights are $\rho_2 = \rho_3 = \rho_4 = \rho_5 = \rho_8 = \rho_9 = 1/2$ with arbitrary surface weights depending on our normalization. If instead we associate a weight 1/2 with each step of the trail then vertex types 2, 3, 4, and 5 have no extra weight while the contact vertex types 8 and 9 have a weight 2. This is then an interacting L-lattice trail with step fugacity 1/2 and with specific bulk and arbitrary surface Boltzmann weights. The subsequent mapping to the Manhattan walk is described by Bradley [6] and the weights thereby obtained are those of a single Manhattan polygon at bulk Boltzmann weight $\omega_b = \sqrt{2}$. This is precisely an interacting Manhattan polygon at the collapse temperature [1]. In a similar manner the dense loop model at $\lambda = \pi/2$ (that is, $n = 0$) is related to fully packed L-lattice trails and hence Manhattan walks.

3.4. Numerical transfer matrix calculations

We have compared the transfer matrix eigenspectra of all four loop and vertex models defined above on finite strips of width up to $N = 6$. For the vertex models, the diagonal-to-diagonal transfer matrices are defined as products of transfer matrices $T_1(u)T_2(u)$ depicted in figure 8. These latter transfer matrices are constructed in the usual way, and for the six-vertex model with weights (3.7), and the 15-vertex model with weights (3.11) are of size $2^N \times 2^N$ and $3^N \times 3^N$, respectively, but break up naturally into sectors.

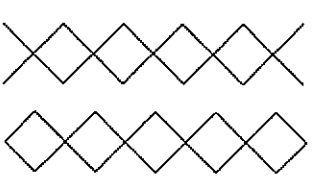

Figure 8. The transfer matrices T_1 and T_2 (T_1 involves only bulk weights), the product of which is defined to be the diagonal-to-diagonal transfer matrix for the vertex models.

The construction of the diagonal-to-diagonal loop model transfer matrix is more involved, and follows similar lines to those in [13] for row-to-row transfer matrices (with periodic boundaries). In both cases, the rows and columns of the transfer matrix are indexed by connectivities. For a given 'diagonal' i of the lattice $\mathcal{L}$ covered by a graph $\mathcal{G}$, the connectivity encodes the way in which some (or none) of the edges of i are covered and the way in which some (or none) of these covered edges are pairwise connected. Details—particularly on the enumeration of connectivities—can be found in [13]. Each connectivity is associated with a number n_d, called 'the number of dangling bonds' and defined to be the number of edges covered by $\mathcal{G}$ but not connected to any other edge. The transfer matrix can be broken up into an even n_d and an odd n_d sector. Furthermore, within each of these sectors the transfer matrix is block upper triangular, reflecting the fact that its application can never increase n_d. Just as with the vertex models, the diagonal-to-diagonal transfer matrix is naturally constructed as a product $t_D(u) = T_1(u)T_2(u)$ of transfer matrices, with matrix elements that can be obtained from the Boltzmann weights using a suitable algorithm.

At the isotropic point of interest ($u = \lambda/2$) we see an exact correspondence between the eigenspectra, up to non-zero multiplicities, of all four models at the appropriate value of $\sqrt{Q} = 2\cos\lambda$. This gives us confidence that our exact calculations for the six-vertex model, for which the solution is at hand, are directly applicable to the related models.

3.5. Bethe ansatz calculations

In [8] the Bethe ansatz solution was used to derive the surface free energy and the leading finite-size correction to the free energy of the six-vertex model on $\mathcal{L}$ for an even number of edges in a row. The reduced free energy, $f_N = -N^{-1}\ln\Lambda_{gs}$, where Λ_{gs} is the largest eigenvalue of the diagonal-to-diagonal transfer matrix $t_D(u)$ with N edges in a row, scales as

$$f_N = f_\infty + \frac{s_\infty}{N} - \frac{\pi\zeta c}{24N^2} + o(N^{-2}) \tag{3.12}$$

in agreement with the expectation from conformal invariance [24]. Here f_∞ is the bulk free energy, s_∞ is the surface free energy, c is the central charge and $\zeta = 2\tan(\pi u/2\lambda)$ is a geometric factor. The bulk free energy is given by

$$f_\infty = -\int_{-\infty}^{\infty} \frac{\sinh(2uy)\sinh[(\pi-\lambda)y]}{2y\sinh(\pi y)\cosh(\lambda y)}\,dy \tag{3.13}$$

and the surface free energy was found to be

$$s_\infty = \ln\left(\frac{\sin[(\lambda+u)/2]}{\sin[(\lambda-u)/2]}\right) - 2\int_{-\infty}^{\infty} \frac{\sinh(uy)\sinh[(\pi-2\lambda)y/2]\cosh[(\pi-\lambda)y/2]\cosh(\lambda y/2)}{y\sinh(\pi y)\cosh(\lambda y)}\,dy. \tag{3.14}$$

We here extend the calculation of [8] in two ways: to any number of edges in a row, and to further correction terms which give the scaling dimensions. Where necessary we refer to equations in that paper with their number prefixed by OB.

Extending the coordinate Bethe ansatz calculation to include an odd number of edges is straightforward. The diagonal-to-diagonal transfer matrix breaks up into sectors which

are conveniently labelled by the number m of down arrows in a row. The Bethe ansatz equations are constructed by an argument which leads from consideration of small values of m to the general case. When $m = 1$, the only equation for the elements of the eigenvectors $F(G)$ of $T_2T_1(T_1T_2)$ that differs is one of the boundary condition equations. If $F(x)$ is the element of F for the down arrow in position x, and $G(x)$ is defined similarly, for an odd number N of edges

$$\Lambda F(1) = w_3^{\mathrm{L}} G(1) \qquad \text{and} \qquad \Lambda G(N) = w_3^{\mathrm{R}} F(N) \tag{3.15}$$

replaces (OB 2.13). When the 'one-body' wavefunctions (OB 2.15) are substituted into the transfer matrix equations, the ratio $B_o(k)/B_e(k)$ obeys the same equations as $A_o(k)/A_e(K)$ does, and it turns out that this ensures that the adapted boundary condition (3.15) gives rise to the same Bethe ansatz equation (OB 2.34).

In the same way, the eigenvector equations for two (or more down arrows) must be adapted from those in [8] if one of the down arrows is at position $x = N$. However, because the eigenvectors are again built from the one-body wavefunctions, the Bethe ansatz equations for the eigenvalues for the case of an odd number of edges are identical to those derived in [8], and given in (3.9), remembering that N may now be interpreted as being odd *or* even.

The largest eigenvalue of the transfer matrix is found in the ground-state sector. The largest eigenvalues in the other sectors Λ_m give further finite-size corrections, which are related to the surface scaling dimensions x^s by [15]

$$\ln \frac{\Lambda_{gs}}{\Lambda_m} \sim \frac{\pi \zeta x^s}{N}. \tag{3.16}$$

The calculation of these eigenvalues by the root density method [25] follows a well trodden path, and so we simply explain the generalization of certain steps in [8].

The equation (OB 3.4) for the root density $\rho_N(\beta)$ must be solved. The standard method converts this to an integral equation of Wiener–Hopf type. The important point is that the condition (OB A3.21) applies only in the sector $m = N/2$ when N is even. In general

$$\int_{-\infty}^{\infty} \rho_N(\beta)\, \mathrm{d}\beta = \frac{1}{\pi}\left[\pi - \lambda + \frac{1}{2N}(1-2m)(\pi - 2\lambda)\right]. \tag{3.17}$$

We then follows the steps in [8] exactly, using the appropriate modification of (OB A3.29),

$$\alpha_m = \frac{(\pi - \lambda)(N - 2m + 1) - \pi}{[2\pi(\pi - \lambda)]^{1/2}}. \tag{3.18}$$

The central charge is then given by

$$c = 1 - 12\alpha_{gs}^2 \tag{3.19}$$

and the scaling dimensions by

$$x_m^s = \tfrac{1}{2}(\alpha_m^2 - \alpha_{gs}^2). \tag{3.20}$$

4. Summary of results and discussion

For the two points of special interest with $u = \lambda/2$, the bulk (3.13) and surface (3.14) free energies reduce to the values

$$\begin{aligned} -f_\infty &= \ln 2 \qquad s_\infty = \ln 2 \qquad \lambda = \pi/3 \\ -f_\infty &= 2C/\pi \qquad s_\infty = \ln(1+\sqrt{2}) \qquad \lambda = \pi/2 \end{aligned} \tag{4.1}$$

where $C = 0.915\,965\ldots$ is Catalan's constant. The values at $\lambda = \pi/2$ are in agreement with the well known results for Hamiltonian walks on the Manhattan lattice [9–11], while the values at $\lambda = \pi/3$ are for the Manhattan ISAW.

Our results for the central charge and scaling dimensions, from equations (3.19) and (3.20), are summarized as follows. For even widths the ground-state sector has equal numbers of up and down arrows, so that $m = N/2$, and the central charge is

$$c^{\mathrm{s,even}} = 1 - \frac{6\lambda^2}{\pi(\pi-\lambda)} \tag{4.2}$$

and the surface scaling dimensions are

$$x_j^{\mathrm{s,even}} = \frac{j}{\pi}[j(\pi-\lambda) - \lambda] \tag{4.3}$$

where $j = N/2 - m$ and $j = 1, 2, \ldots$. These results coincide with those obtained for the $U_q(su(2))$-invariant spin chain [26].

The lowest energy sector for odd strip widths matches as closely as possible the number of up and down arrows, so that $m = (N-1)/2$ and we have the calculated (sometimes called effective) central charge as

$$c^{\mathrm{s,odd}} = -5 + \frac{6\lambda}{\pi}\left(\frac{3\pi - 4\lambda}{\pi - \lambda}\right) \tag{4.4}$$

and the scaling dimensions as

$$x_j^{\mathrm{s,odd}} = \frac{j^2}{\pi}(\pi-\lambda) + \frac{j}{\pi}(\pi - 2\lambda) \tag{4.5}$$

where j now labels the sectors relative to $(N-1)/2$ and $j = 0, 1, \ldots$.

This scenario of different central charge and scaling dimensions depending on whether one uses odd or even strip widths was remarked upon before for periodic boundary conditions (see (2.1), (2.2) and (2.9)).

It would seem peculiar that different strip widths lead to lattice models that are described by different conformal field theories! The explanation is, however, at hand. As for periodic boundary conditions with odd strip widths [27], the lowest energy state from which the central charge and scaling dimensions are calculated is not the true ground state of the system (in the thermodynamic limit) in that it is one of spin 1/2 rather than the spin 0 it should be (and is for even strip widths). This means that the central charge and scaling dimensions calculated for odd strip widths need to be adjusted to give the correct results. (We note that this procedure is trivial at $\lambda = \pi/3$ where all the central charge formulae coincide.)

The adjusted results for the odd strip widths than *fill in* the gaps in the even strip width series. This allows one to write down master formulae combining even and odd strip widths. The central charge is

$$\hat{c} = 1 - \frac{6\lambda^2}{\pi(\pi - \lambda)} \tag{4.6}$$

and the surface scaling dimensions are

$$\hat{x}_k^{\mathrm{s}} = \frac{k}{4\pi}[k(\pi - \lambda) - 2\lambda] \tag{4.7}$$

while for the bulk we have

$$x_k^{\mathrm{b}} = \frac{[k^2(\pi - \lambda)^2 - 4\lambda^2]}{8\pi(\pi - \lambda)} \tag{4.8}$$

with $k = 1, 2, \ldots$ for both series.

We can now compare our $\lambda = \pi/3$ results to those found from work on the equivalent Manhattan ISAW and KGW models [1]. Here the central charge is $\hat{c} = 0$. Our new results (the surface exponents) are in complete agreement with the surface scaling dimension found from numerical simulation of kinetic growth walks and related arguments [1]. These are, in full,

$$x_k^{\mathrm{s}} = \frac{k(k-1)}{6} \tag{4.9}$$

and the smallest of these are

$$x_1 = 0 \qquad x_2 = 1/3 \qquad x_3 = 1 \qquad \text{and} \qquad x_4 = 2 \tag{4.10}$$

which are precisely those given in [1]. An intriguing point is that while these scaling dimensions were found from one set of boundary conditions they relate to two different surface transitions (where the Manhattan walk model has different boundary weights). The explanation of this result lies in the fact that by simply changing the arbitrary surface weights w_s^{L} and w_s^{R} in the six-vertex model we can map our problem to any surface interaction in the Manhattan lattice problem. Hence we must pick up any possible surface scaling dimension. The bulk exponents have already been confirmed [1] and the scaling dimensions are those of the even strip width calculation only (since, as stated previously, the Manhattan lattice does not allow odd strip widths with periodic boundary conditions). Note here that both the bulk thermal and magnetic exponents X_σ and X_ϵ are identified as $x_1^{\mathrm{b}} = 1/4$. We additionally note that (4.9) was also found for an O(n) model on the honeycomb lattice [19].

The other case of interest is $\lambda = \pi/2$ where the six-vertex model can be mapped via the dense loop model to the problem of Hamiltonian walks on the Manhattan lattice. Again the bulk scaling dimensions are only those of the even strip width calculation and are given as

$$x_k^{\mathrm{b}} = \frac{k^2 - 1}{4}. \tag{4.11}$$

Making the same bulk identification here as at $\lambda = \pi/3$ for consistency's sake we have $X_\sigma = X_\epsilon = x_1^{\mathrm{b}} = 0$. Hence the exponents $\nu = 1/(2 - X_\epsilon) = 1/2$ and $\gamma = (2 - 2X_\sigma)\nu = 1$. The central charge is

$$c = -2. \tag{4.12}$$

These exponents agree with the direct exact results of Kasteleyn [9] and Duplantier and David [10, 11]. (Note that there is only one Hamiltonian walk for each rooted Hamiltonian polygon on the Manhattan lattice.)

For the surface case we have, after adjustment,

$$x_k^s = \frac{k(k-2)}{8} \tag{4.13}$$

with the relevant dimensions being

$$x_1 = -1/8 \qquad x_2 = 0 \qquad x_3 = 3/8 \qquad \text{and} \qquad x_4 = 1. \tag{4.14}$$

This result was also found for a honeycomb O(n) lattice model [19].

These results can also be compared to those of the so-called dense walks which have some finite density less than unity (not to be confused with the dense loop model which is, in fact, fully packed). The dense walk problem has the same central charge ($c = -2$) and all the scaling dimensions listed above. However, it also has another infinite series that occurs in the six-vertex model for odd strip widths (after adjustment) with periodic boundary conditions. These extra bulk scaling dimensions cannot occur in the Manhattan problem because of the non-physical nature of those strip widths. The smallest excluded (bulk) scaling dimension is $-3/16$ which in the dense walk problem leads to $\gamma^D = 19/16$.

Just as interesting is a comparison to recently obtained results [28] for Hamiltonian walks on the honeycomb lattice which show a central charge of $c = -1$. This work identified the thermal and magnetic scaling dimensions as being the same as those found here for the Manhattan problem. This is consistent with the conclusions of Blöte and Nienhuis [29] who pointed out that the fully packed and dense walk systems are in different universality classes. (The fully packed, or Hamiltonian, system is effectively frustrated in some fashion and unstable to perturbations.)

Our conclusions then fall in two categories. One concerns the comments above on the process of calculating scaling dimensions from finite-size corrections to the eigenspectrum: in mapping between these models one does not 'lose' any scaling dimensions and one must be careful to calculate everything from the true underlying ground state. The second category encapsulates the results themselves and their specific values for the two polymer physics problems. We have compared (and contrasted) the Hamiltonian walk problem on the Manhattan lattice with dense walks and Hamiltonian walks on other lattices. Importantly, we have confirmed all the surface exponents found from kinetic growth simulations by mapping the seven-vertex Nienhuis loop model on the square lattice to interacting self-avoiding walks on the Manhattan lattice and subsequent exact calculation on the equivalent six-vertex model.

Acknowledgments

The authors take pleasure in thanking U Grimm, P Pearce, T Prellberg and O Warnaar for fruitful discussions, and T Prellberg and O Warnaar for carefully reading the manuscript. We thank B Nienhuis for stimulating this investigation. Three of us (MTB, ALO and CMY) are grateful to the Australian Research Council for financial support.

References

[1] Prellberg T and Owczarek A L 1994 *J. Phys. A: Math. Gen.* **27** 1811
[2] Duplantier B and Saleur H 1987 *Phys. Rev. Lett.* **59** 539
[3] Vanderzande C, Stella A L and Seno F 1991 *Phys. Rev. Lett.* **67** 2757
[4] Stella A, Seno F and Vanderzande C 1993 *J. Stat. Phys.* **73** 21
[5] Bradley R M 1989 *Phys. Rev.* A **39** 3738
[6] Bradley R M 1990 *Phys. Rev.* A **41** 914
[7] Batchelor M T 1993 *J. Phys. A: Math. Gen.* **26** 3733
[8] Owczarek A L and Baxter R J 1989 *J. Phys. A: Math. Gen.* **22** 1141
[9] Kasteleyn P W 1963 *Physica* 29 1329
[10] Duplantier B 1987 *J. Stat. Phys.* **49** 411
[11] Duplantier B and David F 1988 *J. Stat. Phys.* **51** 327
[12] Nienhuis B 1990 *Int. J. Mod. Phys.* B **4** 929
[13] Blöte H W J and Nienhuis B 1989 *J. Phys. A: Math. Gen.* **22** 1415
[14] Duplantier B 1990 *Phys. Rep.* **184** 229
[15] Cardy J L 1987 *Phase Transitions and Critical Phenomena* vol 11, ed C Domb and J L Lebowitz (New York: Academic)
[16] Duplantier B and Saleur H 1989 *Phys. Rev. Lett.* **62** 1368
[17] Warnaar S O and Nienhuis B 1993 *J. Phys. A: Math. Gen.* **26** 2301
[18] Baxter R J, Kelland S B and Wu F Y 1976 *J. Phys. A: Math. Gen.* **9** 397
[19] Batchelor M T and Suzuki J 1993 *J. Phys. A: Math. Gen.* **26** L729
[20] Sklyanin E K 1988 *J. Phys. A: Math. Gen.* **21** 2375
[21] Destri C and de Vega H J 1992 *Nucl. Phys.* B **374** 692
[22] Yung C M and Batchelor M T 1995 Integrable vertex and loop models on the square lattice with open boundaries via reflection matrices *Nucl. Phys.* B (to appear)
[23] Warnaar S O 1994 Private communication
[24] Blöte H W J, Cardy J L and Nightingale M P 1986 *Phys. Rev. Lett.* **56** 742
[25] de Vega H J and Woynarovich F 1985 *Nucl. Phys.* B **251** 439
[26] Saleur H and Bauer M 1989 *Nucl. Phys.* B **320** 591
[27] Alcaraz F C, Barber M N and Batchelor M T 1988 *Ann. Phys., NY* **182** 280
[28] Batchelor M T, Suzuki J and Yung C M 1994 *Phys. Rev. Lett.* **73** 2646
[29] Blöte H W J and Nienhuis B 1994 *Phys. Rev. Lett.* **72** 1372